Semester project report

Characterization of BlueMUSE FM1 mechanism

Aurélien Genin

Master Student in Robotics

2025 H2

aurelien.genin@cube-monde.net

Supervisor:
Diane Chapuis
EPFL/LASTRO/Astrobots
diane.chapuis@epfl.ch

Professor supervisor:
Jean-Paul Kneib
EPFL/LASTRO
jean-paul.kneib@epfl.ch

Abstract

The Astrobots group of the LASTRO at EPFL is involved in the engineering of the future BlueMUSE integral field spectrograph instrument that will equip the VLT, by designing motorized mounts for the FM1 folding mirrors. These mounts shall make the mirror move in tip and tilt, with a one-shot repeatability precision of $< 5''$ and by retaining a stability of $< 5''$ when subject to $\pm 2°\mathrm{C}$ temperature variations.

A prototype of the mechanism for FM1 has been devised and assembled. This project tackles its characterization regarding both stability and repeatability aspects. For this, an improved optical test bench is set up. A thermal enclosure and control circuit are also developed and assembled to control the temperature around the mechanism and assess the thermal stability. The motion repeatability is tested using limit switches, with a focus on the analysis of backlash and parasite motions inside of the mechanism.

The thermal stability is found to not reach the required value, although issues with the tests and results hint at the possibility of making the mechanism compliant with few modifications. On the other side, the motion is shown to be very repeatable, with a precision over ~ 10 cycles of $< 1''$.

Table of contents

1 Introduction 4
1.1 BlueMUSE instrument 5
1.2 FM1 mechanism 7
1.3 Project objectives 8
2 Stability 9
2.1 Experimental setup 9
2.1.1 Auto-collimator 10
2.1.2 Test enclosure 11
2.1.3 Thermal control 12
2.2 Measurements and results 13
2.2.1 Test bench stability 14
2.2.2 FM1 stability 16
2.2.3 Thermal stability 18
3 Repeatability 21
3.1 Backlash characterization 21
3.1.1 Full-range range 22
3.1.2 Zoom in on the backlash region 23
3.2 Mechanism flexure 25
3.2.1 Measurements 27
3.2.2 Interpretation and consequences 28
3.3 Homing 28
3.3.1 Homing strategy 28
3.3.2 Motion repeatability with homing 30
3.3.3 Control strategy 31
3.4 Installation and calibration reflexion 32
4 Tip-stage assembly 33
5 Conclusion 34
References 35

1 Introduction

To study the Universe in all its greatness, astronomers use many different types of instruments. Although telescopes fit the common sense of “instruments”, for large observatories, the instruments are what is placed at the end of a telescope. With this definition, the telescope is the tool that catches light from sources of interest in the sky and focuses it, and the instruments are what analyse this light. In observational astronomy, these instruments are often classified in three categories: astrometry, photometry and spectrometry. Figure 1 presents these categories and how different instrument types are placed inside.

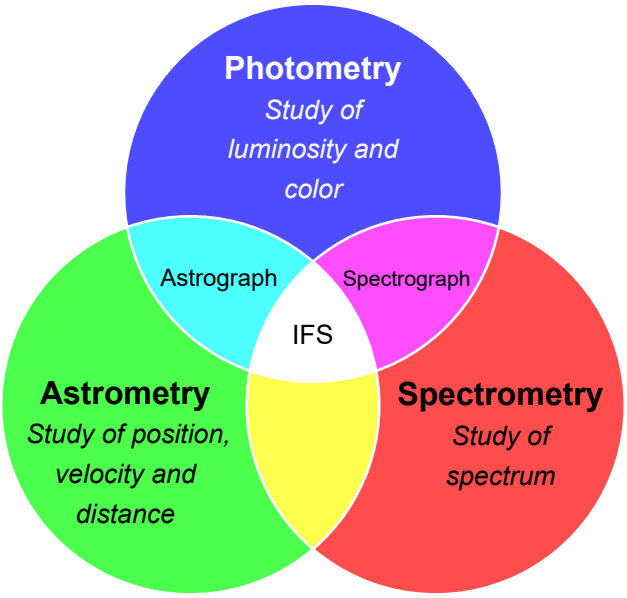

Figure 1: The three main categories of observational astronomy instruments and some examples of instruments types.

From the three main categories, it is possible to conceive instruments that perform multiple types of studies. For example, an astrograph generally consists of a simple camera sensor at the focal plane of a telescope, in order to produce a 2D image. In that case, the instrument records spatial information (astrometry) as well as brightness data on each pixel (photometry).

As can be seen in Figure 1, the pinnacle of astronomical instruments is an

Integral Field Spectrograph (IFS)[1]. Indeed, an IFS produces a cube of data containing spatially-resolved spectral data. In other words, it produces an image where each pixel contains a full spectrum. This is particularly useful to study galaxies as it allows to look at the spatial distribution of specific chemical elements in them. Figure 2 shows a graphical example of the data produced by an IFS.

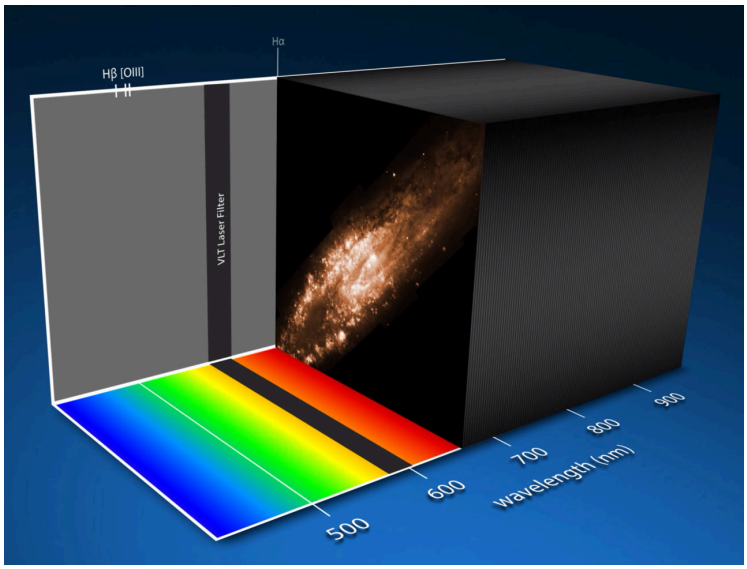

Figure 2: Cross section of a cube of data produced by the IFS MUSE at the VLT. It shows part of the Hα band in the Sculptor galaxy revealing the galaxy rotation. (Credit: ESO/L. Calçada/E. Congiu et al. [1])

1.1 BlueMUSE instrument

The best integral field spectrograph currently in the world is the Multi Unit Spectroscopic Explorer (MUSE) installed at the Very Large Telescope (VLT) [2]. The VLT is a set of four main 8.2m telescopes from the European Southern Observatory (ESO) located at the Paranal site, in the Atacama desert in Chile. Thanks to its image quality and throughput, MUSE is a tremendous success in the astronomical community and has been used in many papers, such as a detailed study of the Sculptor galaxy in the full visible spectrum (shown in Figure 2) [1].

Built on the heritage of MUSE, BlueMUSE is a new integral field spectrograph that has been selected by ESO as part of the VLT2030 instrument

[1] An IFS is not always the best instrument depending on the observation, for technical, financial and availability reasons. However, in theory, getting spatial, luminosity and spectral data is always better than only two out of three.

suite to improve current VLT instruments. Its main objective is to extend the limitations of MUSE in terms of wavelength and spectral resolution by covering the near-UV and blue part of the spectrum: 350-580nm at a spectral resolution $R > 2600$ (average $R = 3500$ over the wavelength range) [3], [4]. Figure 3 shows the comparison of the BlueMUSE and MUSE spectral resolution and wavelength range.

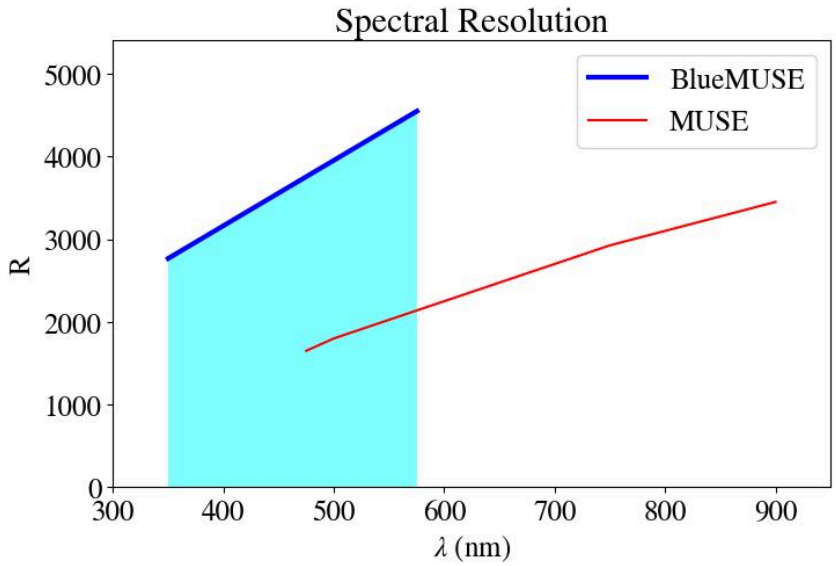

Figure 3: Comparison of the BlueMUSE (in blue) and MUSE (in red) spectral resolution and wavelength range [3].

Furthermore, BlueMUSE will have a field-of-view of $1' \times 1'$ and a spatial sampling of $0.2 - 0.3''$, with a peak throughput of $\sim 35\%$, similar to MUSE in the red part of the spectrum. BlueMUSE is expected to start its operations in 2031 at the VLT, and will largely contribute to the global knowledge in astronomy, especially about the local volume, the nearby galaxies and the distant universe [4].

The following video[2] from ESO presents the optical design of MUSE, which is very similar to the one of BlueMUSE. The light entering the instrument is first reshaped, then cut in 24 slices (16 for BlueMUSE) that will each follow identical paths. Each slice is then further splitted into 48 beams before being sent to a spectrograph that disperses the light according to its wavelength. These 48 spectrums are then recombined on a camera sensor, and then numerically assembled with the spectrums from the 23 others slices. This data is then processed to package it as a proper cube of data, such as the one shown in Figure 2.

[2] https://www.youtube.com/watch?v=-fh2Y6Zyhwc&t=379s

1.2 FM1 mechanism

BlueMUSE is developed by an international consortium, led by CRAL (Centre de Recherche Astrophysique de Lyon). EPFL is part of the consortium through the LASTRO (Laboratory of Astrohysics), and especially the Astrobots engineering group. It is responsible for the design of the automated relay optics alignment, namely the FM1 and FM2 mirrors of the instruments.

These mirrors are folding mirrors that redirect the light in each of the 16 identical optical paths to keep the instrument compact. The experience of MUSE showed that they moved slightly (a few arcseconds) out-of-alignment with seasonal temperature variations. This required to manually re-adjust them to reach the peak performance of the instrument. The goal for BlueMUSE is therefore to motorize the mounts of the FM1 and FM2 mirrors to enable performing these corrections remotely and more frequently.

A first prototype mechanism for FM1 has been developed at Astrobots [5]. It uses two motors to move the mirror with 2 degrees-of-freedom, namely tip and tilt rotations as can be seen on Figure 4.

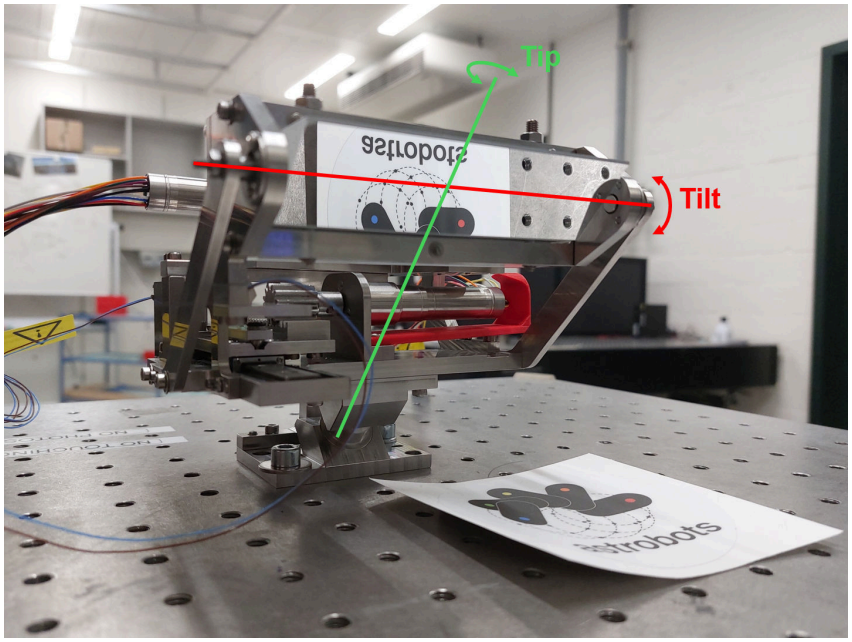

Figure 4: FM1 mirror mechanism prototype actuable in tip (green) and tilt (red).

The motion of the mirror must be very fine, with a complete motion range of only $5'$ and an accuracy of $5''$. To reach this precision, the rotation from the motor is converted to a linear motion with a rack-and-pinion mechanism (1), which moves a carriage (2). This carriage holds a slope, tilted using a fine shim to produce a tilt of only 0.15mm of height over 64mm of

length. A ball bearing contacts this slope (3) and moves a lever arm that is directly connected to the mirror, creating the rotation (4). Figure 5 shows the actuation of the tilt axis and the different steps in the motion conversion and transmission. This mechanism gives a theoretical transmission ratio of $\eta = \theta_{\text{motor}}/\theta_{\text{mirror}} = 0.153''/\text{ rad}$ where θ_{motor} is the motor rotation before its reducer (the one sensed by the encoder in the rotor) and θ_{mirror} is the mirror rotation (here, in tilt) [6]. The mechanism for the tip axis is very similar, with only the lever arm being different.

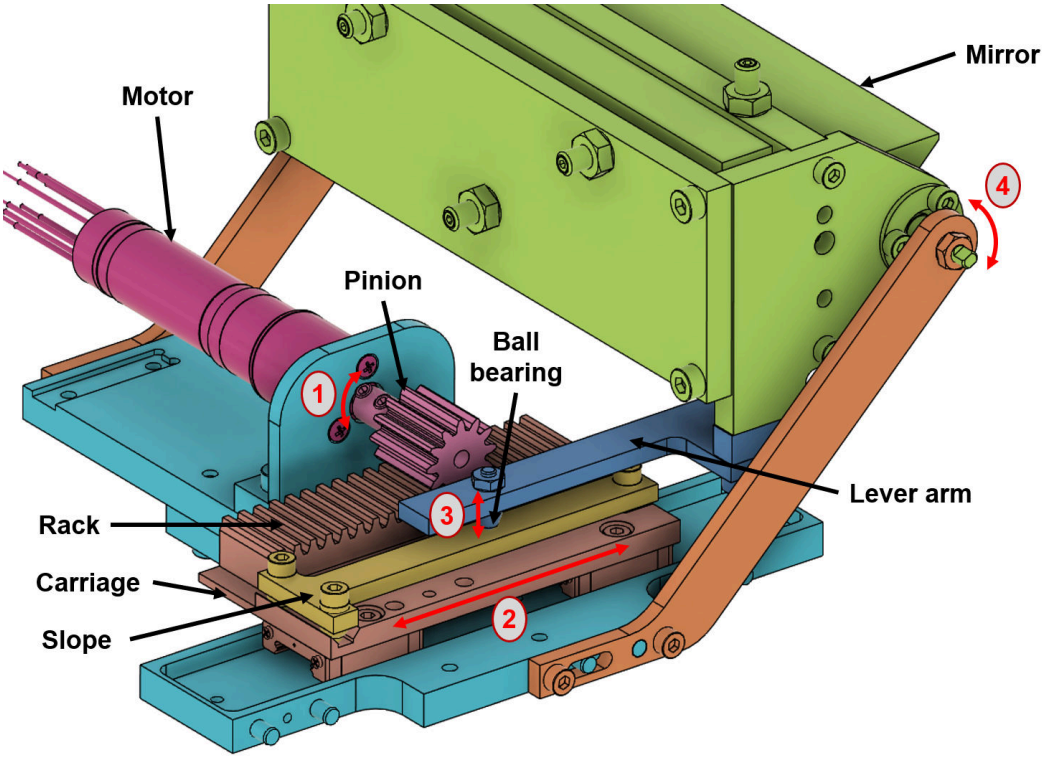

Figure 5: 3D view of the FM1 tilt mechanism showing the names of the different parts, as well as the different steps in the motion conversion and transmission.

1.3 Project objectives

As presented before, the FM1 mechanism is currently at the prototype level and is being assessed to decide if it can be used in the final instrument. The goal of my project was therefore to characterize the prototype and quantify its performances. The objectives of my work were the following:

- Characterization of the mechanism stability
  - Install a new test bench with an auto-collimator for the mechanism

  - Develop and test a test bench to measure the thermal stability of the mechanism
  - Measure and quantify the stability of the mechanism
- Characterization of the mechanism repeatability
  - Measure and understand the backlash in the mechanism
  - Install limit switches on the mechanism and test the homing procedure
  - Quantify the mechanism repeatability
- Assembly of the tilt axis

This report presents my work regarding these objectives and the results I have obtained. Section 2 details the work done regarding the stability of the mechanism, Section 3 is about the characterization of the mechanism repeatability, and Section 4 presents the assembly and initial tests of the tip axis. Most of my work is focused on the tilt axis as the tip axis has been assembled only towards the end of my project.

2 Stability

This section focuses on the characterization of the FM1 mechanism stability. The stability is defined as the time evolution of the mirror angle, relative to its base, when the mechanism is not actuated. Here, we don't care about the absolute angle between the mirror and the base, but only its relative evolution. Moreover, this relative evolution is generally composed of two terms: a drift (long-term evolution) and a noise (short-term evolution). This section presents results and analysis of these two components.

The FM1 mechanism has to follow the following requirements regarding stability, from the BlueMUSE system engineering team [5]:

- **The FM1 mechanism shall maintain a stability of $< 5''$ on its tilt (resp. tip) axis.**
- **The FM1 mechanism shall maintain its stability requirement when subjected to a temperature variation of $\pm 2°\mathrm{C}$ over a course of 12h.**[3]

2.1 Experimental setup

To measure the stability of the FM1 mechanism regarding these requirements, we have used the general test bench shown in Figure 6. This setup

[3] This requirement is called "thermal stability" throughout this report.

is an improvement from the one used for preliminary tests, and presented in [6]. It consisted of a single laser source that was separated by a beam splitter. One beam reflected on a fixed flat mirror before going back to the beam splitter and towards a camera to serve as a reference beam. The other beam was reflected on the FM1 mirror towards a folding mirror that sent the beam back to the FM1 mirror and towards the beam splitter and eventually to the same camera as the reference beam to serve as the test beam. The resulting video feed from the camera showed two light dots and their relative motion was directly giving the motion of the mirror. However, this setup proved to not be stable enough given the small angles that had to be measured, hence the improved one.

2.1.1 Auto-collimator

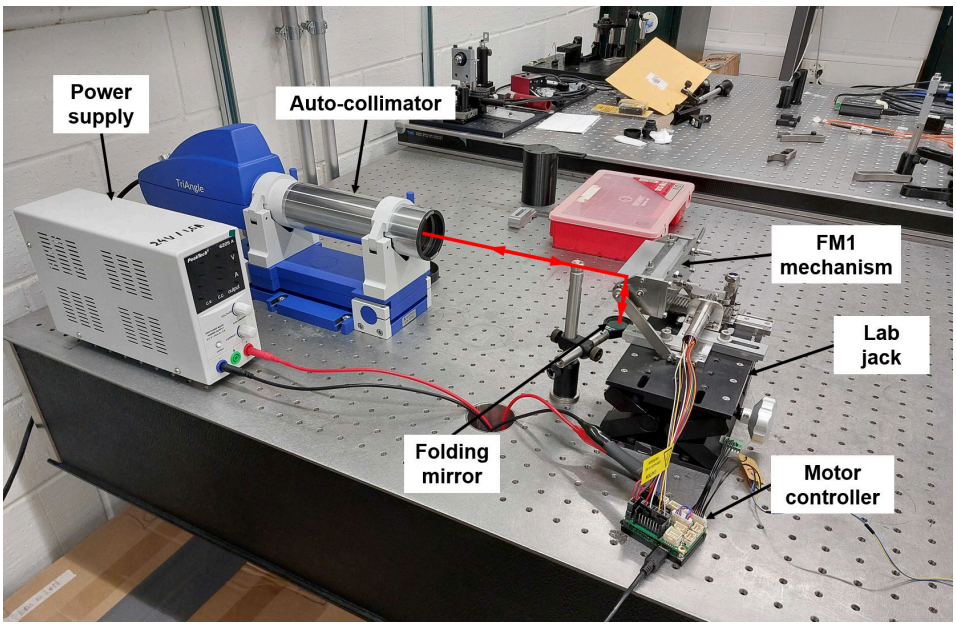

Figure 6: Test setup for the FM1 mechanism with an auto-collimator. The light beam path from the auto-collimator is drawn as a red line.

To solve this issue, a new test bench has been devised using an auto-collimator to measure the angle of the mirror. The auto-collimator sends a single beam of light that is reflected on the FM1 mirror, on a folding mirror, and then back on the FM1 mirror towards the auto-collimator. The latter measures the angle difference between the initial beam and the returning beam.

As shown in Figure 7, the angle measured by the auto-collimator is not directly the angle of the mirror. It actually depends on the number of reflections of the beam. In a standard use case, with a flat mirror (a), the measured

angle is twice the angle of the mirror from the reference. For this reason, the software of the auto-collimator already halves the angle α and therefore returns directly $\theta = \alpha/2$.

In our test setup (b), the beam is reflected twice on the test mirror. Therefore, the angle measured by the auto-collimator is 4 times the actual angle of the mirror (from its $45°$ reference). Since the auto-collimator already divides α by 2, we still have to divide by 2 the angle returned by the auto-collimator to retrieve the mirror angle. **For this reason, all measurements from the auto-collimator in this setup are divided by 2.**

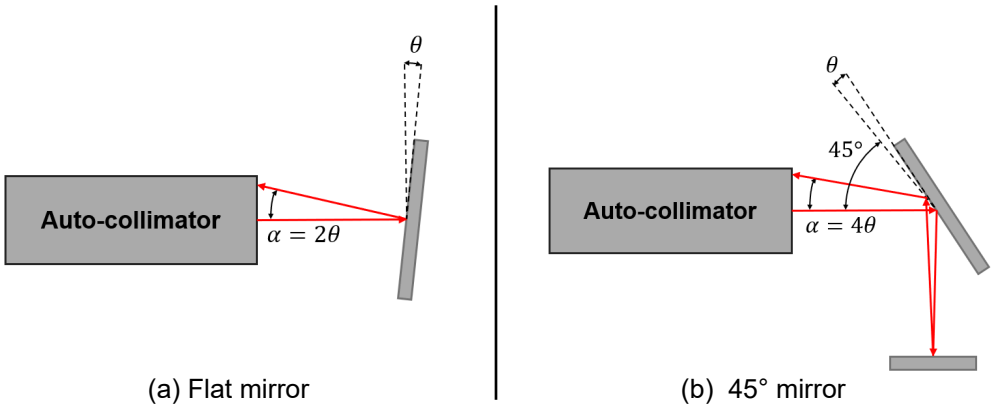

(a) Flat mirror (b) 45° mirror

Figure 7: Schematic of the auto-collimator measurements in two mirror setups.

2.1.2 Test enclosure

Initial tests with this new setup have shown some variations because of temperature fluctuations (more on this in Section 2.2.3). Moreover, since we need to characterize the stability of the mechanism when it is subjected to temperature variations, it is required to have a way to control the temperature around the FM1 mechanism.

For this, the chosen solution was to install an enclosure around the mechanism. This enclosure serves as a thermal chamber in which the temperature can be controlled. However, it needs to be transparent (at least on the mirror side) so that the beam from the auto-collimator can still pass through.

A first idea was to use the laboratory's thermal chamber for this. However, the temperature changes required for the tests ($4°\mathrm{C}$ variations) were deemed too small for it. Additionally, it was being used at the time of my project.

Instead of buying an expensive commercial thermal enclosure, I built a simple test enclosure out of laser-cut acrylic. The final enclosure can be seen

in Figure 8. The different sides were attached using tape instead of glue to avoid clouding of the acrylic that would have reduced the transparency. The bottom side was kept clear to allow to simply place the enclosure on top of the mechanism on the table. Finally, a small notch has been cut on one of the side to pass the cables of the motor controller.

Figure 8: Test enclosure made out of laser-cut acrylic

2.1.3 Thermal control

To quantify the FM1 mechanism thermal stability, it is necessary to be able to raise the temperature around the mechanism by $4°\mathrm{C}$. The test enclosure presented above is meant to contain the heat. An electric circuit was devised to be able to heat up the inside of this enclosure, as well as control the temperature. Figure 9 presents the electrical circuit used.

The circuit is controlled by an Arduino UNO microcontroller. It controls two 6W electric heaters by switching on or off a relay. These heaters are simply resistive wires housed in an aluminum casing to distribute the heat. To measure the temperature, a DS18B20 temperature sensor is wired to the Arduino board, which has a resolution of $0.06°\mathrm{C}$ (12 bits)[4].

It is therefore theoretically possible to use the temperature sensor to control the temperature inside the enclosure in closed-loop, and to follow a pre-

[4] Its accuracy is given to be $0.5°\mathrm{C}$ but that is the absolute accuracy, not the resolution. In our case, we care more about the resolution than the absolute accuracy since the goal is to measure relative temperature variations.

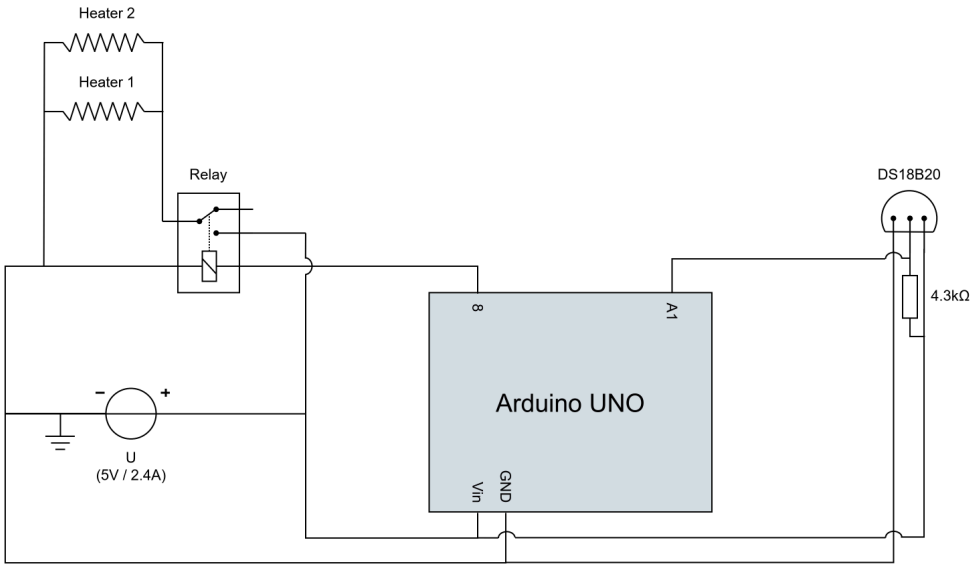

Figure 9: Circuit diagram of the thermal control system used for the stability tests.

programmed slope of $+4°C$ over 12h. However, this part of the code has not been implemented for practical reasons encountered during the tests (detailed in Section 2.2.1). For the following thermal stability tests, the program followed a fixed 6h 50% duty cycle for the heaters (i.e. the heaters are powered on fully during 3h, then powered off for 3h, and this cycle is repeated).

Since the Arduino UNO can't store data by itself, the temperature inside the test enclosure is logged using the portable thermometer of the laboratory that is placed inside the enclosure during the tests. It has a resolution of $0.1°C$ and records it only every 30min. This is not an ideal solution, but was sufficient for these tests.

2.2 Measurements and results

This section presents the results of the stability tests for the tilt axis of the FM1 mechanism. In order to make sure our measurements are sound and trustworthy, the stability of the test bench alone has first been measured (Section 2.2.1). This gives a reference to compare the results of the FM1 tests. The stability of the mechanism has also been tested with and without the thermal control and test enclosure.

2.2.1 Test bench stability

To measure the stability of the test bench alone, the idea is to simply move the folding mirror in front of the FM1 mirror to directly reflect the beam of the auto-collimator to it, as can be seen on Figure 10. Because the beam only reflects once on the mirror, the measurements from the auto-collimator are not halved, following the explanation given in Section 2.1.1.

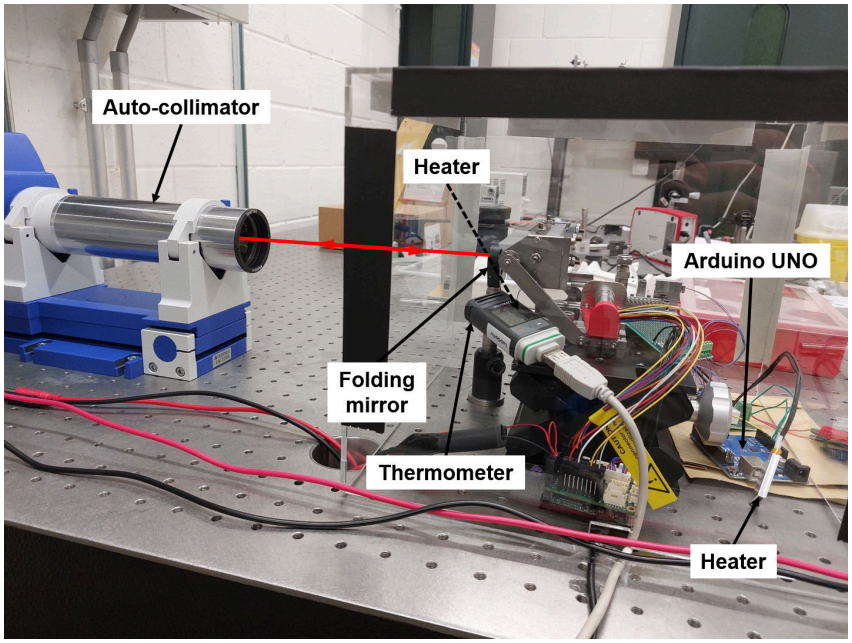

Figure 10: Test setup to measure the stability of the test bench. The light beam path from the auto-collimator is drawn as a red line. One heater can't be seen in the image but has been indicated with a dotted line.

With this setup, the thermal stability of the test bench has been measured over 17h, with measurements from the auto-collimator saved every 1s. The results are shown in Figure 11. To better understand the data, the signal is decomposed as the sum of a mean motion and a noise. The mean motion is computed as the rolling average of the signal, with a sliding window of 60 data points (i.e. 1min). The noise is then computed as the residue of the signal minus the rolling average.

This method decouples the noise from the mean motion for better clarity. It can then be observed that the 3σ-noise of this setup is $0.30''$ along the X axis (horizontal) and $0.29''$ along the Y axis (vertical). These values are one order of magnitude lower than the $5''$ requirement for the stability, and therefore make it theoretically possible to measure the mechanism stability and validate this requirement.

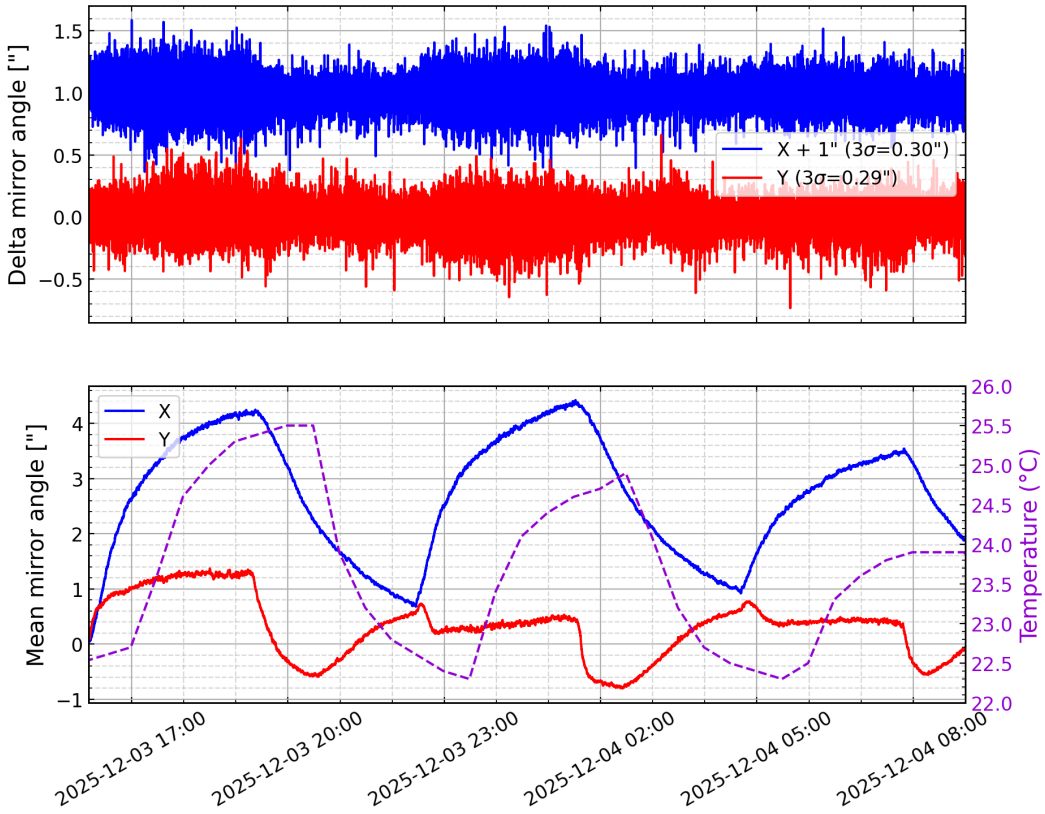

Figure 11: Thermal stability of the test bench. The bottom figure shows the mean motion of the setup (1min rolling average), the top figure shows the noise. The X axis shows horizontal motion of the beam, the Y axis shows vertical motion.

A frequency analysis, using a Fast Fourier Transform (FFT), of this noise signal reveals a mostly white noise as the energy spectrum is mostly flat (see Figure 12). Only a large peak at 5.6h is observed. It is the period of the temperature control circuit. It should in theory be 6h, but the time is measured quite imprecisely by the Arduino UNO, leading to this drift.

Looking at the bottom graph in Figure 11 reveals first that the temperature variations are only of $3°\mathrm{C}$. This is likely caused by the inefficiency of the radiative heat-up from the heaters. Indeed, the heaters are placed on their corner on top of the optical table to minimize the heat transferred by conduction. If heat were transferred by conduction through the table, it would create temperature gradients that would result in warping of the table and therefore motion of the test bench. Apart from this minimal conductive transfer to the table, most of the heat transfer is therefore conductive transfer to the air, and then convection inside the thermal enclosure. However, the thermal conductivity of air is notoriously low ($0.026.\mathrm{W.m^{-1}.K^{-1}}$), making the heat

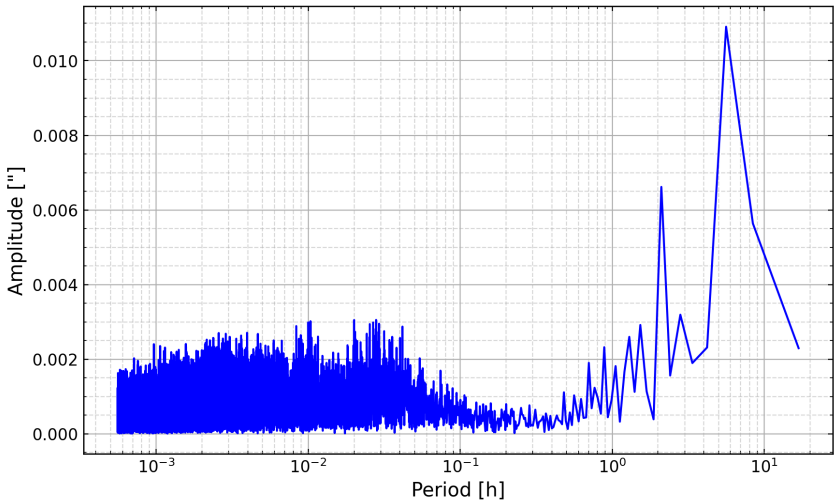

Figure 12: FFT of the X noise in the thermal stability test of the test bench.

transfer from the heater to the air very inefficient (hence the common use of radiators to increase the surface area).

Finally, the mean motion reveals large variations of $4''$ in X and $2''$ in Y. These are obviously correlated with the temperature variations, and reveal that the test bench is sensible to temperature. Given that these variations are in the same order of magnitude as the stability requirement for the mechanism, it means that **all following stability measurements are too be taken with care because it is not possible to separate motions coming from the FM1 mechanism from motions of the test bench with full certainty**.

Figure 13 shows the result of another stability test of the test bench, without the temperature control circuit, over the course of 144h (6 days) at a sampling period of 10s. The temperature variations are therefore natural variations (e.g. when people entered or left the room), and of much smaller amplitude. The 3σ-noise appears smaller at only $0.11''$ and $0.15''$ but this is likely caused by the lower temperature variations as Figure 11 showed that the noise is also correlated with temperature. The mean motion also presents the same correlation, with an amplitude similar to the one observed in the other thermal stability test.

2.2.2 FM1 stability

The stability of FM1 has been first quantified without the test enclosure and the thermal control circuit. The test bench is therefore identical to the one pictured in Figure 6. The results of a stability test carried over 137h (5.7 days) are shown in Figure 14.

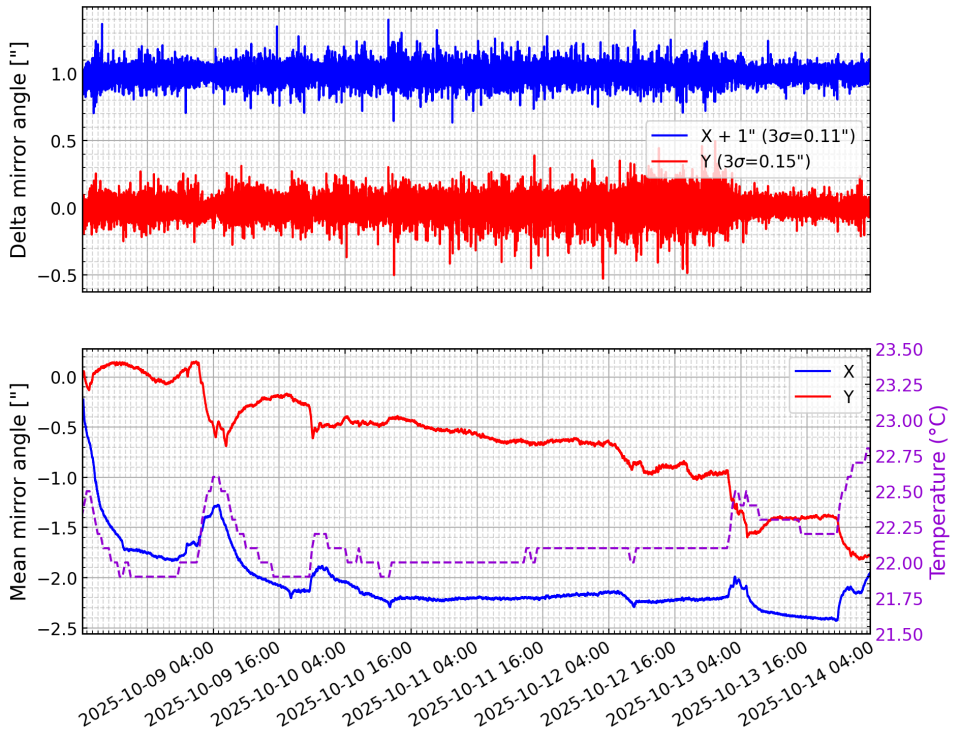

Figure 13: Stability of the test bench without thermal control over 144h.

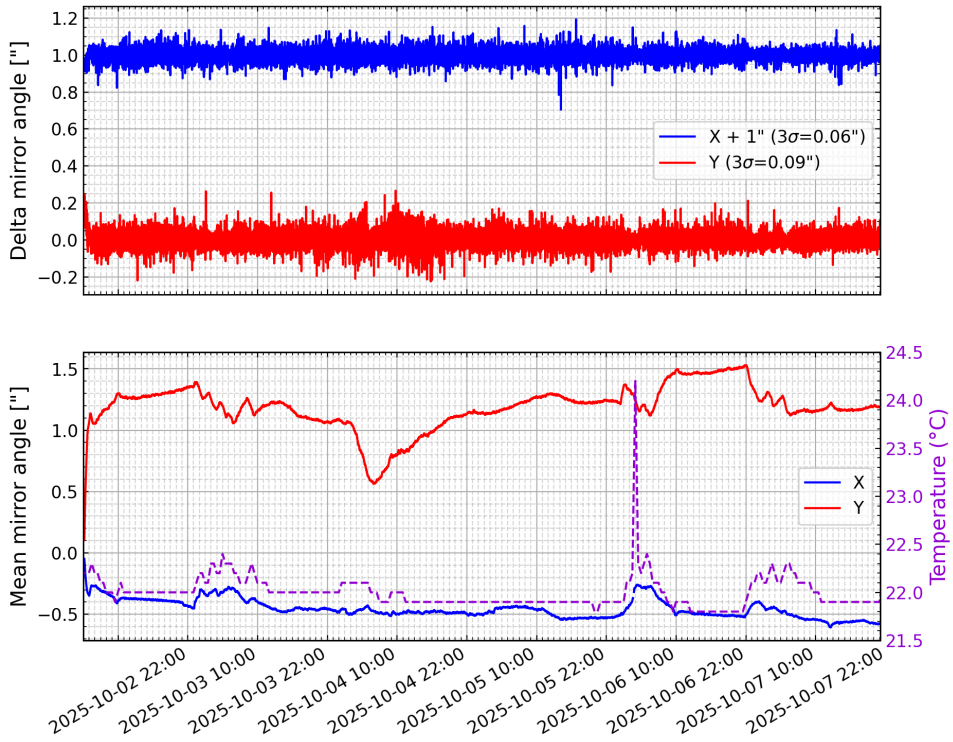

Figure 14: Stability of the FM1 mechanism without thermal control over 137h. The bottom figure shows the mean motion (10min average), the top figure shows the noise. The X axis shows tip motion of the mirror, the Y axis shows tilt motion

Figure 14 reveals a story similar to the test bench stability test carried in the same conditions (Figure 13). It is to be noted that the angles in Figure 14 have been divided by 2, which was not the case in Figure 13. This is a consequence of the double reflection on the FM1 mirror explained in Section 2.1.1. By keeping this in mind, we see that the 3σ-noise is identical in both experiments, and therefore entirely caused by the test bench (likely measurement noise from the autocollimator as it is specified for an accuracy of $0.75''$). Regarding the mean motion, we observe a similar correlation between mirror motion and temperature. The amplitude appears larger on the Y axis (tilt axis), but this is likely a coincidence and no solid conclusion can be drawn out of it.

On this long test, with minimal temperature variations ($0.5°\mathrm{C}$), we observe that the first stability requirement is met since the mirror stays stable at $< 1.5''$. Although this is only a preliminary result, it is reassuring and shows that the mechanism is capable of holding the mirror with the required very fine stability.

2.2.3 Thermal stability

To further investigate the thermal stability of the FM1 mechanism, and try to validate the second stability requirement, the mechanism has been placed inside the test enclosure with the thermal control circuit. The setup is therefore very similar to the one showed in Figure 10, with the only exception of the folding mirror no longer being in front of the FM1 mirror (like in Figure 6). The thermal stability test with FM1 has been carried only over 5h with the two heaters because of lack of time.[5] The results are shown if Figure 15.

Regarding the 3σ-noise, it is very similar to the one observed with only the test bench, with values of $0.19''$ in the X axis (tip) and $0.24''$ in the Y axis (tilt). As before, this noise is mostly caused by the test bench, and very likely by the auto-collimator.

The mean motion reveals a more dramatic story. With a temperature amplitude of $3.5°\mathrm{C}$, the mirror shows a maximum tilt motion of $9.5''$, outside of the stability requirement, and a tip motion of $1''$. This large motion can be explained by multiple factors.

First, as presented in Section 2.2.1, the test bench is itself sensible to temperature variations. It is therefore very likely that part of the motion observed

[5] Some tests have been carried out with only one heater, which showed only a $2°\mathrm{C}$ temperature amplitude.

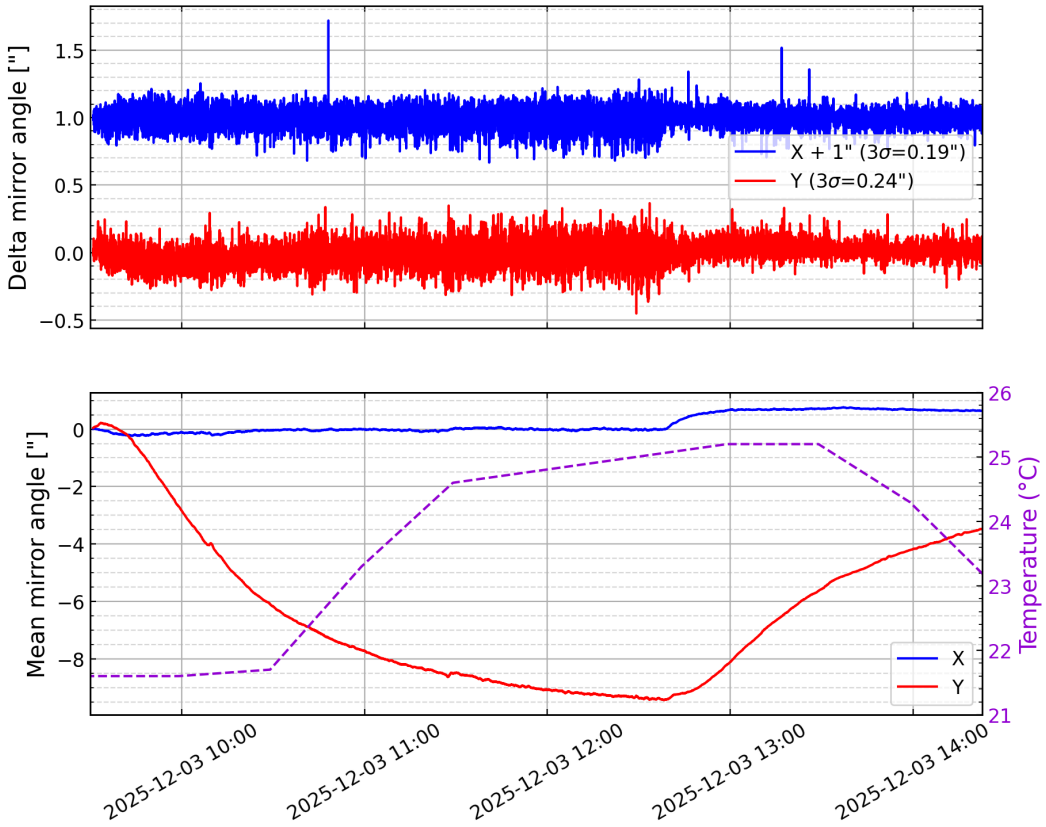

Figure 15: Thermal stability of the FM1 mechanism over 5h. The bottom figure shows the mean motion (1min rolling average), the top figure shows the noise. The X axis shows tip motion of the mirror, the Y axis shows tilt motion.

with FM1 are in fact caused by the test bench. A strange phenomenon that we can observe is the fact that we don't recover here the $4''$ motion in X that was present in the test bench thermal stability results (Figure 11). This might imply that there was something wrong in one of these tests.

Another issue with the test bench is the temperature inhomogeneity. The heat transfer inside the test enclosure mostly happens through convection. However, this convection is only natural and not forced (with fans for example). Therefore, the temperature takes a long time to settle, and creates gradients. This effect can be seen in Figure 15 and Figure 11 by the time lag between the maxima/minima of mirror motion and the maxima of temperature. An attempt to mitigate this effect was made by placing the two heaters at opposite corners of the enclosure, however this reveals insufficient. It could be interesting to place multiple thermometers inside the enclosure to quantify this effect.

Furthermore, even though I tried to minimize the thermal transfer via conduction through the table, it is likely that some still happens. If this transfer happens, it could create temperature gradients in the lab jack holding the mechanism, and in the structure of the FM1 mechanism, resulting in warping and parasite mirror motion. This effect should be measured by placing temperature probes on the FM1 mechanism. Ideally, this data could also be used to calibrate a thermal simulation of the mechanism to better understand how it behaves with temperature variations. Indeed, it is still unclear how the mechanism heat-up will happen in the BlueMUSE instrument. For these tests, we assumed that it would come from the air around the mechanism. However, it could also come from the instrument structure and therefore arrive to the FM1 mechanism from its base, leading to temperature gradients.

A source directly within the FM1 mechanism that could explain the large motion observed on the tilt axis is the material of the slope. For this test, a glass slope was used (contrary to the test presented on Figure 14 which used a steel plate). The whole mechanism is made of steel, which should prevent deformations because all parts have the same thermal expansion coefficient. However, with a glass slope, this hypothesis is broken. The culprit might even be the glue bonding the glass slope to the steel carriage. If the glue (or the glass slope) expands differently that the structure, it could make the ball bearing in the mechanism drift slightly vertically and move the mirror along the tilt axis. That would explain the large motion in the tilt axis, and the smaller one in the tip axis (the tip stage was not mounted for this test).

Finally, to increase the temperature variations amplitude up to $4°\mathrm{C}$, multiple solutions could be explored:

- Insulate the thermal enclosure, e.g. by wrapping it in aluminum foil to better keep the heat inside
- Improve the air heat-up by installing radiators on the heaters
- Improve convection by adding a fan

As a conclusion, these tests are not enough to statute on the thermal stability requirement. **They show that the stability is at least in the same order of magnitude as the requirement.** However, work is still to be done to stabilize the test bench itself, and ensure that no deformations happen in the FM1 mechanism (due to temperature gradients, or different expansion coefficients).

3 Repeatability

The second aspect of the characterization of the FM1 mechanism is its repeatability. It is about the ability of the mechanism to reach a mirror position with high accuracy and precision. The accuracy refers to the average error to an absolute position target. The precision is the deviation around the average position for multiple attempts at reaching the same target. In the case of FM1, the requirement about repeatability for BlueMUSE is the following [5]:

- **The FM1 mechanism shall reach a target position with a precision of $< 5''$ in one shot.**

The requirement isn't *per se* concerning the absolute accuracy as it will be more of a matter of installation and calibration (more on this topic in Section 3.4).

An important aspect of the requirement is the fact that the target must be reached in one shot. This is a major difference with the previous work [6]. Before, the position of the mirror (measured by the position of the beam using the camera, similar to what is doing the auto-collimator in the new test bench) was used to create a closed-loop control for the mechanism. Therefore, the mechanism performed in average 2-3 motions to reach the target position with the required $5''$ accuracy and precision. However, it has been clarified by the BlueMUSE team that this will not be feasible in practice. Indeed, the correction to be applied to FM1 will be computed by simulating the whole instrument to identify performance losses and corrections to apply to the different elements. This process will take a long time and can not be used to apply a closed-loop control for the FM1 mechanism.

For this reason, my work has been focused on characterizing and testing the one-shot repeatability of the FM1 mechanism. The following sections present the different results regarding backlash, flexure, homing and calibration.

3.1 Backlash characterization

Usually, the main source of non-repeatability in a mechanism is backlash. It is generally caused by gears that require some play to mesh properly. However, when the motion of the gears is reversed, this play creates a period where the gears un-mesh before re-contacting on the opposite side.

This effect creates an hysteresis cycle when looking at the output shaft position of the mechanism versus the input shaft: it is called backlash.

In the FM1 mechanism, backlash is present inside the motor reducer (specified for $1.3°$ [6], equivalent to $0.81″$ on the mirror) and more importantly at the rack-and-pinion. This section presents tests and results to visualize and understand this backlash.

3.1.1 Full-range range

The first idea to visualize and quantify backlash is to make the mechanism move back-and-forth over its full range of motion. Such a test should result in a clean hysteresis cycle where the offset between the forward and backwards journey is the backlash.

The setup for these tests is the one shown in Figure 6. The mirror angle (here, in tilt) is measured by the auto-collimator, directly with its proprietary software (TriOptics), and divided by 2 afterwards. The motor position is measured by the encoder positioned on the motor shaft (before the reducer), with the software given with the controller (EPOS Studio).

Figure 16 presents the result of three tests of full-range motion to visualize the hysteresis. A linear reference is added by drawing a straight line from the origin position to the furthest position. It reveals a slight curvature in the motion conversion. This effect was already documented in [6] and is caused by the flexure of the slope in the mechanism: because the slope flexes in the middle where it isn't supported, the ball bearing sits lower than it should be. This effect was present with the steel slope (used for the tests shown here) and the glass slope. To cancel it, new slopes made out of ceramic will be installed.

The figure also presents a significant jitter. This is caused by the surface roughness of the slope. We also realized that the ball bearing is not rolling on the slope but is actually sliding. This digs a groove in the steel slope and disturbs the measurements.

Finally, Figure 16 reveals the backlash of the full mechanism. It appears as the offset between the forward journey (top part of the figure) and the return journey (bottom part of the figure). When the motion is reversed (at the top left of the graph), the backlash creates a difference in position of the mirror for a same position of the motor.

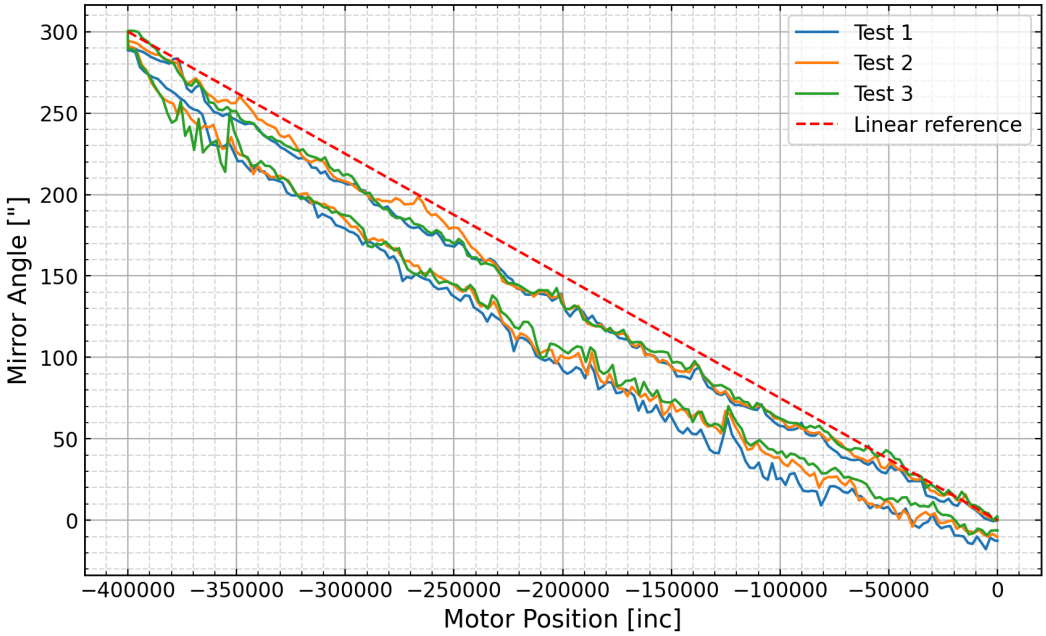

Figure 16: Backlash visualization over the full range of motion of the tilt axis of the FM1 mechanism. Three identical tests are shown. A linear reference (red dotted) is added.

This effect is further revealed in Figure 17 where the linear reference is subtracted from the measurements to focus on the deviation form the linear motion. The curvature is also made more obvious. In this figure, the backlash can be measured to be $\sim 30''$. For reference, the slope and lever geometries result in a motion conversion of $5.9''/\ \mathrm{mm}$ from the carriage linear motion to the mirror rotation. The backlash observed on the mirror would therefore represent a backlash of $\sim 5\mathrm{mm}$ on the carriage (in the rack-and-pinion). This is a lot more than what is visually observed and that the play necessary for such gears. It indicates that the backlash observed here is more complex. It is however to be noted that the backlash looks very repeatable in these tests. It is therefore theoretically possible to calibrate the mechanism to suppress it through the controller, for example by adding an offset in the motor position when it changes of direction.

3.1.2 Zoom in on the backlash region

To better understand what is going on with the backlash, I performed tests at a smaller scale. Instead of moving the mechanism over its full motion range, the idea was to zoom in on the backlash region. The tests therefore consisted in realizing small motions (27,000 encoder increments = $\sim 6\%$ of the full motion range). They were also done at lower speeds (10rpm instead

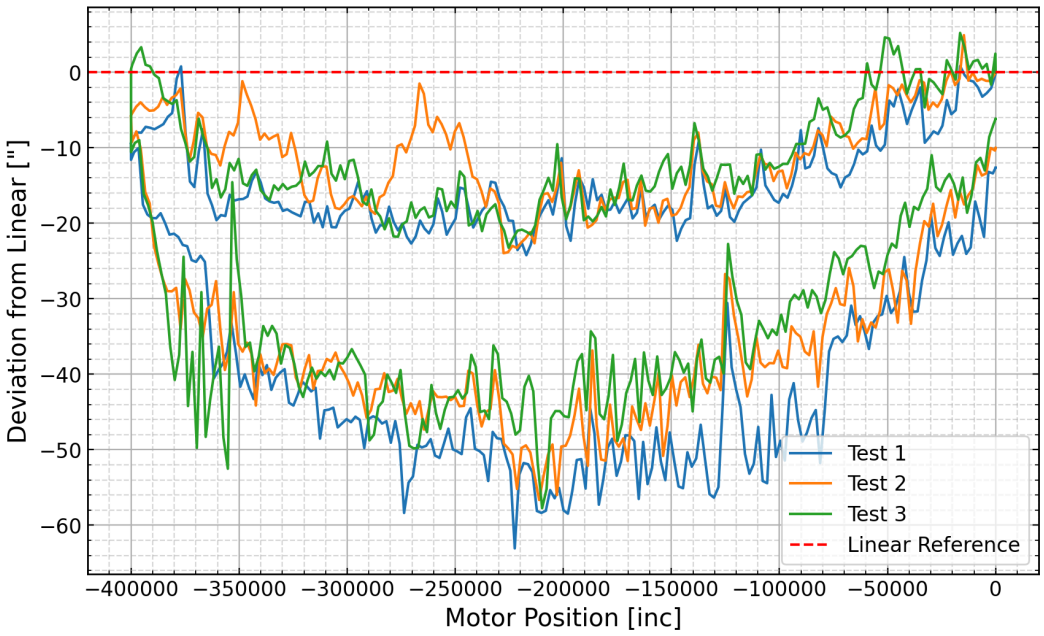

Figure 17: Deviation from the linear reference over the full range of motion of the tilt axis of the FM1 mechanism. Three identical tests are shown.

of 500rpm for the motor, before the reducer) to minimize the effect of surface roughness. To observe the backlash, the mechanism was first moved in the positive (resp. negative) direction and the test was executed by moving in the negative (resp. positive) direction.

Figure 18 shows an analysis of such a test. As commanded, the motor position follows a constant linear slope. However, multiple phases can be observed in the motion of the mirror. The linear motion is the normal motion conversion performed by the mechanism. It is jagged because of the surface roughness, as was shown in Figure 16.

The backlash is observed when the mirror is not moving but the mirror is. It is measured to take 4500 encoder increments. Given the mechanism conversion rate of $0.00187''/\text{ inc}$, **this backlash is equivalent to an error of $8.4''$ on the mirror position, or 1.4mm on the carriage position (more consistent with the tolerance in the rack-and-pinion)**.

However, Figure 18 reveals two additional phases. I called them “release” and “pick-up” in an attempt to give a physical interpretation for them. Section 3.2 details the investigation of these phases, but the following should be taken with care as it is still an hypothesis to be fully confirmed. Here is a possible physical interpretation for these two phases:

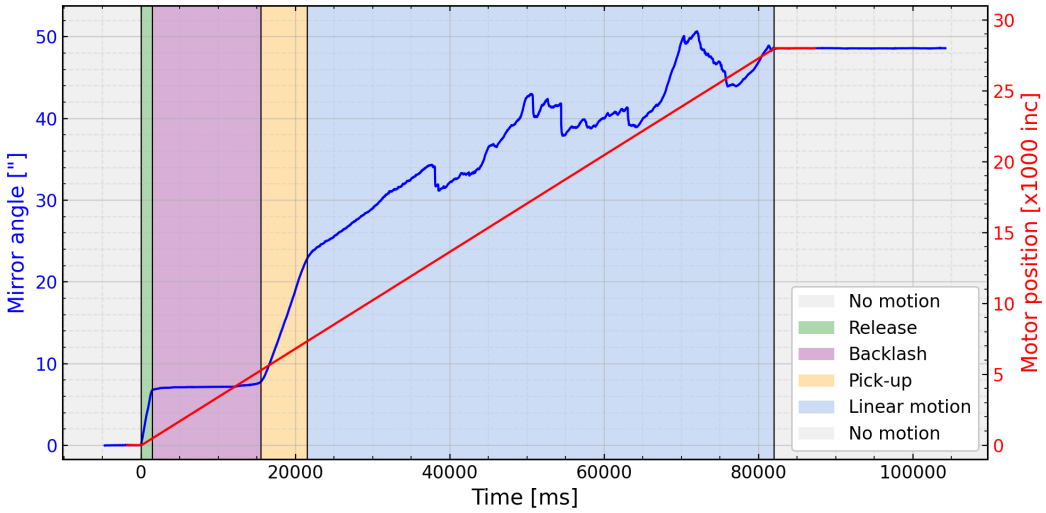

Figure 18: Analysis of the zoom in on the backlash region. Different phases of the motion are indicated as colored regions.

- Because the ball bearing doesn't roll on the slope, it creates a substantial static friction. This friction transmits horizontal forces from the slope to the ball bearing. These forces load the mechanism over multiple possible locations: mis-alignment of the rack and pinion gear forcing a twist of the carriage, play in the bearings holding the mirror, flexures of the structural parts…
- When the motion is reversed, the forces vanishes and the mechanism is unloaded making it move to its resting position (reached when the gears of the rack-and-pinion un-mesh). This is the "release" phase.
- When the gears of the rack-and-pinion re-mesh on the other side, the mechanism is first loaded before being actually put in motion. This is the "pick-up" phase.

It is to be noted that this backlash region ("release" + "backlash" + "pick-up" phases) is very repeatable. The amplitude of the "release" and "pick-up" phases are not the same when the motion is reversed from positive to negative or from negative to positive. However, the total amplitude of the backlash region stays the same at $\sim 7,000\text{inc}$ on the encoder or $\sim 24''$ on the mirror. These arguments are consistent with the proposed physical interpretation.

3.2 Mechanism flexure

To test the physical interpretation of the "release" and "pick-up" phases, multiple tests have been performed.

This was also motivated by a second anomaly observed and shown on Figure 19. It shows the result of a simple back-and-forth motion executed ~10 times to test the repeatability of the homing calibration (more on this in Section 3.3). In this test, the FM1 mechanism is actuated only in the tilt axis. However, it can be seen that the mirror also moves in the tip axis. This creates another hysteresis cycle:

1. The mirror moves in tip and tilt simultaneously,
2. The mirror moves only in tilt (the slight drift in tip is likely caused by the mirror not being perfectly perpendicular with the auto-collimator),
3. When the motion is reversed, the mirror first moves in tip and tilt simultaneously,
4. The mirror moves only in tilt.

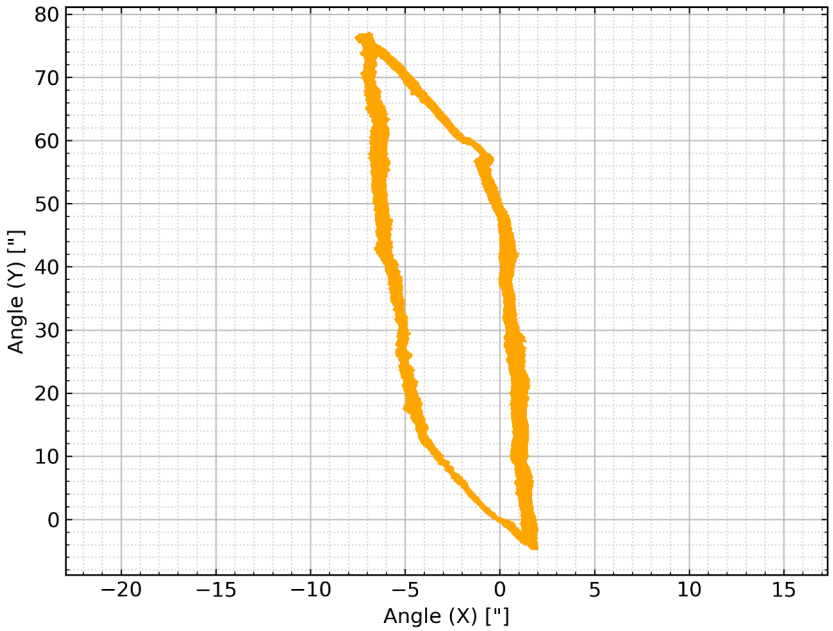

Figure 19: Mirror motion in tilt (Y) and tip (X) over multiple homing sequences followed by a 50,000inc motor movement in tilt. The scales in X and Y are different.

What is even more interesting is that the phases where the mirror moves in the parasite direction (here, in tip) exactly coincide with the backlash region ("release" + "backlash" + "pick-up" phases) previously presented. This indicates that the "release" and "pick-up" phases and this parasite motion are linked. Furthermore, the hypothesis explaining the "release" and "pick-up" phases as flexure in the mechanism would also explain this parasite motion: if the mechanism were to flex (due to play in the joints or flexures in the parts), it would move the mirror not purely in tilt, but very likely also in tip, creating the observed parasite motion.

3.2.1 Measurements

To verify this hypothesis, the idea is to measure the absolute motion of the mirror through the backlash region. This is performed by commanding the FM1 mechanism to move by +10,000inc through backlash. The position of the mirror cage is probed using a comparator positioned at different locations. The comparator is set to zero before the mechanism motion and recorded after the motion. This process is illustrated on Figure 20. The measurements are summarized in Figure 21.

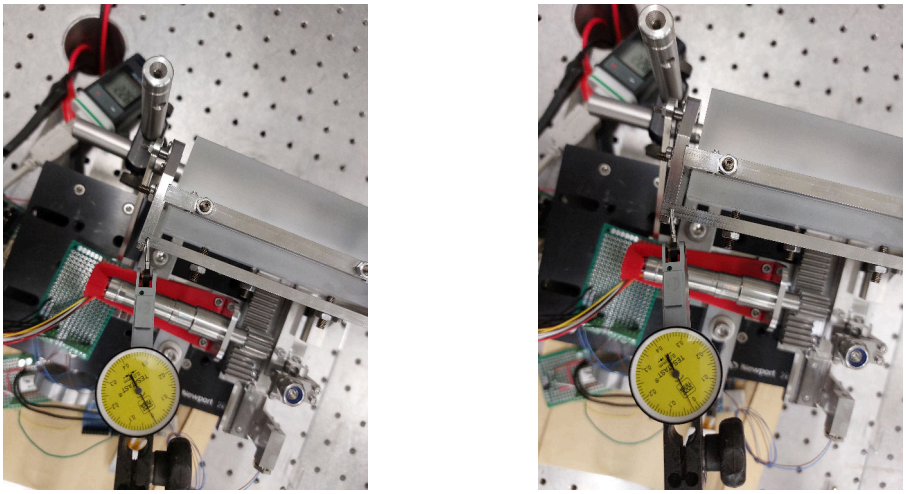

(a) Before motion (b) After motion

Figure 20: Photographs showing the measurement process of the mirror absolute motion through backlash.

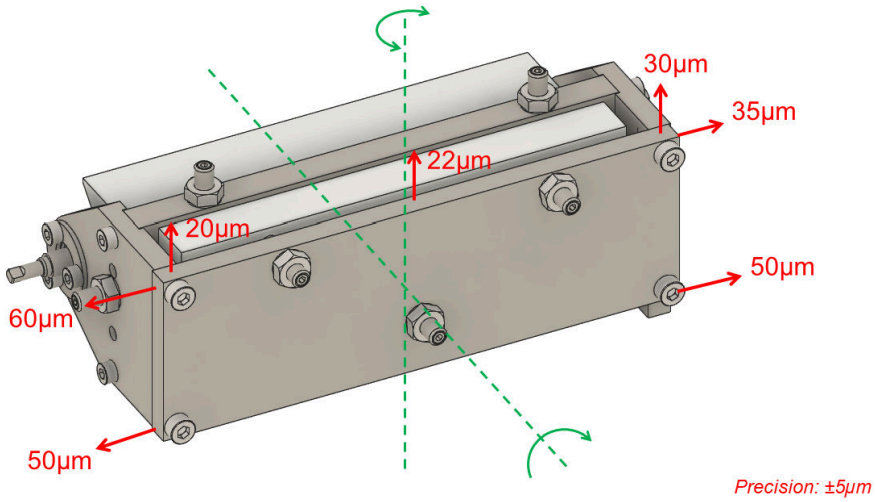

Figure 21: Absolute motion of the FM1 mirror cage when the mechanism is moved by +10,000inc through backlash. Green lines indicate possible rotations explaining the measured displacements.

Figure 21 shows the absolute motion of the mirror cage after a movement of +10,000inc through backlash. From these measurements, the existence of a parasite motion becomes obvious. The uneven motion of the top side of the mirror cage are likely a result of the vertical rotation of the mirror. The opposite motion of the lateral sides of the mirror can only be explained by an horizontal rotation of the mirror (as it would not make sense for the cage to expand).

3.2.2 Interpretation and consequences

Although these parasite motions seem minuscule, they have a direct impact on the repeatability of the mechanism since the requirements are so tiny. Given that the distance between mirror tilt pivot shaft and the mirror back side is 41.2mm, a mirror rotation of $5''$ induces a rise of the mirror back side of $1.0\mu\text{m}$, to be compared with the $20 - 30\mu\text{m}$ observed in Figure 21.

These measurements have highlighted the presence of a parasite motion in the mechanism and support the physical interpretation of the “release” and “pick-up” phases as internal motion in the mechanism. **More measurements like these ones should be performed in other location in the mechanism (all over the mirror, on the carriage, near the ball bearing…) to better understand how the FM1 mechanism moves.**

3.3 Homing

Even though the previous sections aiming at suppressing the backlash through control have shown that this task is much harder than expected, another option is available to reach the required repeatability. This section presents the implementation and testing of homing (the process of calibrating a zero-position, usually with limit switches) on the tilt axis of the FM1 mechanism and how it can be used to reach a precision with $1''$ repeatability in one-shot.

3.3.1 Homing strategy

An improvement on the FM1 mechanism added during my project is the installation of two limit switches on the tilt axis (two other limit switches are also present on the tip stage). They can be observed on Figure 22. They are connected to the motor controller with a custom electric board I soldered which simply wires the limit switches to the standard connector for the

controller, with $150\,\mathrm{k}\Omega$ pull-up resistors[6].

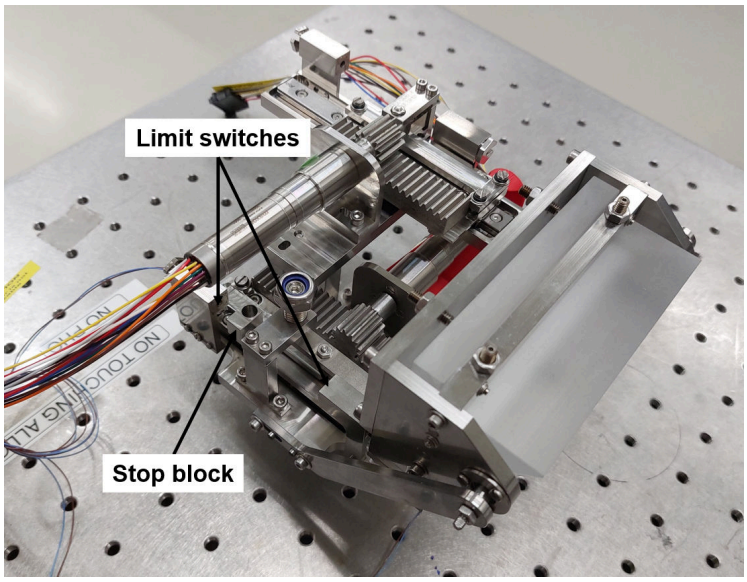

Figure 22: Position of the limit switches and stop block on the tilt axis.

The EPOS Studio software used to control the motor comes with multiple algorithms for homing [7]. The one I used is the “Negative Limit Switch & Index” homing sequence. Figure 23 presents how it works. In this sequence, the controller moves towards the limit switch in the negative direction with a speed called “swift search speed”, until the limit switch is contacted. Then, it reverses its motion and moves in the positive direction with a speed called “zero search speed”, until the limit switch is released. At this point, the home position is referenced and set. A final optional step makes the motor continues to move in the positive direction (with the swift search speed) a set number of increments to move away from the limit switch and avoid triggering it by mistake. The same sequence exists with the positive limit switch.

This homing sequence is very robust for two main reasons. First, the zero search is usually done at a much smaller speed than the swift search. This minimizes the brake distance and ensures that the edge of the limit switch is precisely located. Secondly, **because the motion is reversed directly in the homing sequence, the backlash is already suppressed**. It is for

[6]This wiring makes it so that when a limit switch is not contacted, the motor controller sees a positive voltage. When the limit switch is contacted by the stop block, the voltage drops to zero. This has however the disadvantage of starting the controller in fault state, which is resolved by switching the activation state of the switches in EPOS Studio. This is because the controller automatically stops every motion of the motor if the limit switches are triggered outside of a homing sequence, for safety.

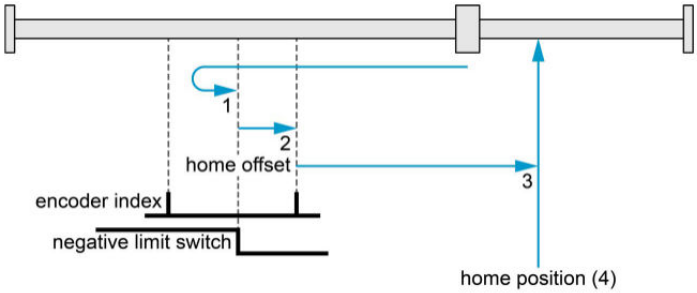

Figure 23: Schematic of the "Negative Limit Switch & Index" homing sequence [7].

this reason that it is not necessary to be able to suppress the backlash in the control (more details in Section 3.3.3).

3.3.2 Motion repeatability with homing

The repeatability of the homing has been tested by performing multiple homing sequences consecutively, with an additional 50,000inc motion after the homing (equivalent to $\sim 80''$ on the mirror). These tests were performed with a swift search speed of 100rpm and a zero search speed of 10rpm. The results are shown on Figure 24.

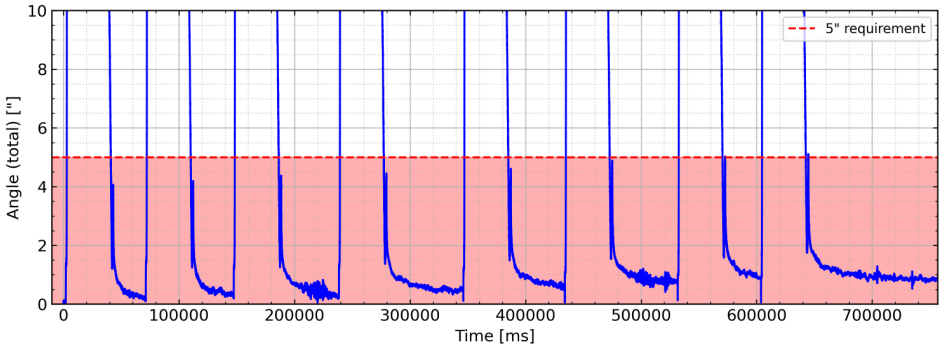

Figure 24: Repeatability of the tilt axis of the FM1 mechanism with a set target of 50,000inc after homing on the negative limit switch. The mirror angle is the total angle (tip and tilt). The $5''$ requirement threshold is shown in red.

It can be seen that the FM1 mechanism is very repeatable over these 8 cycles, with an ability to reach its target with a maximum error of only $1.0''$, much lower than the $5''$ requirement. This repeatability can also be observed on Figure 19 which shows separately the tip and tilt motion of the mirror over these same 8 cycles. The repeatability is therefore shown as the thickness of the line as each cycle overlaps with the others.

The only issue observed in these repeatability tests with homing is a slight drift of the error after multiple cycles. This can be seen on Figure 25, where

the target is always reached slightly further at each new cycle. The direction of this drift is consistent with the ball bearing sitting every time a bit lower. A plausible explanation is therefore that the ball bearing or the slope wears slightly during the travel from the target position to the limit switch and back, and this wear is enough to make the ball sit slightly lower, and therefore make the mirror slightly miss its target. As an order of magnitude, given the lever length of $82\mathrm{mm}$, an error on the mirror angle of $1''$ is caused by an error on the altitude of the ball bearing of only $0.4\mu\mathrm{m}$. As a reminder, the total slope changes the altitude of the ball bearing by $150\mu\mathrm{m}$. Another fact reinforcing this wear hypothesis is that this drift was much more pronounced with the steel slope than with the glass slope, as the steel is more easily marked by the hardened ball bearing. For this reason, **all repeatability tests shown here have been carried out with the glass slope**.

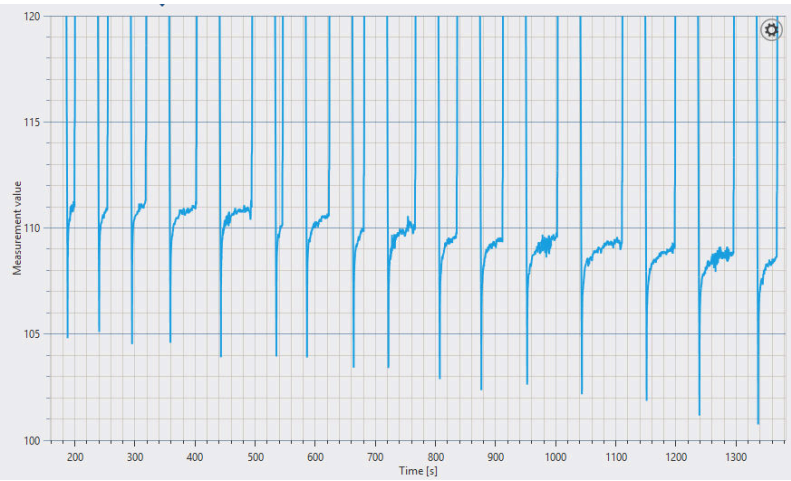

Figure 25: Drift of the repeatability error after multiple cycles. The angle value here show only the Y axis (tilt) and have not been divided by 2 (they show twice the mirror angle).

3.3.3 Control strategy

As presented before, the FM1 mechanism displays very good one-shot repeatability when the backlash is eliminated with homing. Moreover, the mechanism will have to perform corrective motions inside the instrument at most once a day and will have multiple hours to do so. It is therefore possible to implement a slow and non-reactive control strategy for the FM1 mechanism.

The best option for this control then seems to be the following. To reach a new target angle for the mirror, the mechanism performs a homing sequence followed immediately by a defined motion, as demonstrated in Section 3.3.2.

The distance of this motion (in motor increments) could be determined theoretically, given the known conversion ratio of the mechanism. However, a more precise way is certainly to use a look-up table. For this, the mechanism is commanded to sweep over the full motion range (similarly as in Figure 16), after a homing sequence, and the position of the mirror and the motor are record to form the look-up table. Then, when a specific mirror target angle is given, the table can be used to determine the equivalent number of motor increments.

Currently, given the surface roughness of the slope, this method might not be precise enough. However, with the future ceramic slope, it should be possible to implement. Hopefully, these ceramic slopes should also solve the wear issue and therefore the look-up table should remain stable in time.

3.4 Installation and calibration reflexion

This section delves into how the FM1 mechanism will be installed in the BlueMUSE instrument and the following steps to ensure proper accuracy. In operations inside the BlueMUSE instrument, the FM1 mirror will have to move to a precise absolute position with respect to the base of the mechanism. All the work presented here only focused on the repeatability in the sense of the precision or relative accuracy. However, there is currently no way to know the absolute position of the mirror (i.e. if it is at $45.0°$ with respect to its base or $44.9°$).

To reach absolute position accuracy requires two elements:

1. Precise relative position control of the mirror (this is the topic of the previous section)
2. Precise knowledge of the absolute mirror position when the mechanism is in a reference position (e.g. when the tip and tilt axis are at one of the limit switches)

For the second point, an accurate metrology setup and procedure will have to be devised to measure precisely the absolute mirror position with respect to the FM1 base (with an accuracy $< 5''$) and/or to set precisely the mirror position (e.g. with adjustments in the ball bearing height). Adding adjustability to the mechanism will make it possible to calibrate all 16 FM1 mechanism at the exact same angle to simplify the control. However, this adjustability will have to be locked very tightly once the calibration is performed to avoid it to drift with time.

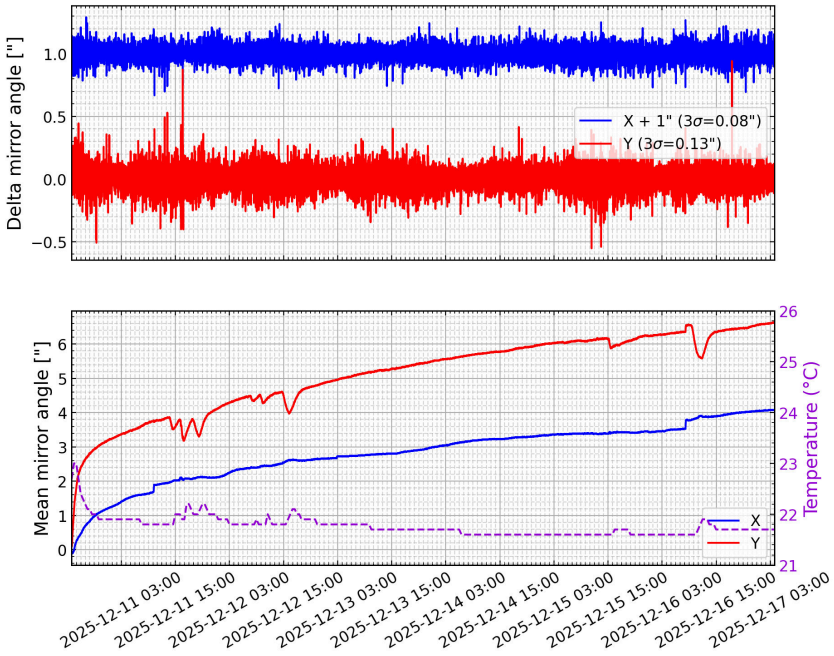

Figure 26: Thermal stability of the FM1 mechanism with tip and tilt axes over 156h. The bottom figure shows the mean motion (5min average), the top figure shows the noise. The X axis shows tip motion of the mirror, the Y axis shows tilt motion.

4 Tip-stage assembly

Throughout my time working on this project at Astrobots, new parts for the FM1 mechanism were being manufactured. These new parts were mostly for the tip stage. Indeed, most of the work and results presented in this report only showed performances of the tilt axis of the mechanism. Over the end of my project, the tip axis was ready to be assembled. Figure 5 shows the full mechanism with both axes of motion mounted.

Although not a lot of tests has been carried out with this configuration because of a lack of time, Figure 19 and Figure 24 show repeatability results of the tilt axis when the mechanism's tip axis was installed (although not actuated).

Figure 26 presents preliminary stability results with both axes installed. This test was carried over 156h (6.5 days), without the thermal enclosure and control circuit. A continuous drift in both tip and tilt axes can be observed throughout the course of the test. The conclusion on this test is not clear because of this drift that is not seen in previous similar tests on the tilt axis alone. This result is very preliminary, and it would be advisable to re-do a proper thermal stability test before giving any conclusion about it.

Assembling the FM1 tip stage revealed a couple of difficulties that could be addressed in the design for a future version of the mechanism:

- Pin holes are very tight, and some pins were impossible to install (or are impossible to remove if required to disassemble the mechanism).
- Screws to fix the base to the table are very hard or impossible to access to tighten them.
- Limit switch holder bolts on the tip axis collide with the tip carriage in certain position, blocking the mechanism.
- Ball bearings in tip and tilt stages have no adjustability to set the zero position of the mirror. Currently the zero position of the mirror is therefore extremely dependant on the real thickness of the slopes. This will become an even bigger issue with the future thicker ceramic slopes.

5 Conclusion

This work presented the results of the characterization of the current FM1 mechanism prototype. This included thermal stability and motion repeatability. A new optical test bench for the mechanism has been devised and installed, with an auto-collimator for more accurate measurements of the mirror angles, and a thermal enclosure and control circuit to change the temperature around the mechanism. The thermal stability of the mechanism has been assessed, with a maximum tilt motion of $9.5''$ for a temperature change of $3.5°\mathrm{C}$, although this result is plagued with thermal instabilities of the test bench and other issues explained in more details in the report. Even though this result is outside of the stability requirement, it hints at the possibility of achieving it, with proper corrective work on the test bench, and maybe mechanism. Regarding the one-shot motion repeatability, it has been demonstrated with $< 1''$ by using limit switches and a proper homing sequence. Some parasite motions have been revealed and will require further investigation, but the result is very encouraging. Finally, the second axis of motion (in the tip direction) has been installed, opening the door for future tests in both directions. Along with this, future works on repeatability includes the realization of a motion look-up table to reach any mirror position in one shot from a limit switch.

References

[1] E. Congiu *et al.*, “The MUSE view of the Sculptor galaxy: Survey overview and the luminosity function of planetary nebulae,” *Astronomy&Astrophysics*, vol. 700, p. A125, Aug. 2025, doi: 10.1051/0004-6361/202554144.

[2] R. Bacon *et al.*, “The MUSE second-generation VLT instrument,” Nov. 2022, doi: 10.1117/12.856027.

[3] J. Richard *et al.*, “BlueMUSE: Project Overview and Science Cases,” June 2019, doi: 10.48550/ARXIV.1906.01657.

[4] J. Richard *et al.*, “The Blue Multi Unit Spectroscopic Explorer (BlueMUSE) on the VLT: science drivers and overview of instrument design,” June 2024, doi: 10.48550/ARXIV.2406.13914.

[5] D. Chapuis Kerouanton and M. Galal, “BlueMUSE Folding Mirrors Design Description,” techreport BMU-69, Jan. 2025.

[6] A. Nicollier, “BlueMuse FM1 Prototype : Tests, results and improvements.” 2025.

[7] Maxon, “EPOS4 Application Notes,” techreport rel8760, Nov. 2019.